

# Correlatively Coded OFDM

Char-Dir Chung, *Senior Member, IEEE*

**Abstract**—A class of correlative codes is proposed to significantly improve the spectral performance of the rectangularly pulsed orthogonal frequency-division multiplexing (OFDM) signal with or without cyclic prefix or zero padding. It is analytically shown that the correlatively coded OFDM signal can achieve very high spectral efficiency while yielding an extremely small fractional out-of-band power.

**Index Terms**—Orthogonal frequency-division multiplexing, correlative coding, cyclic prefix, zero padding, spectral efficiency.

## I. INTRODUCTION

ORTHOGONAL frequency-division multiplexing (OFDM) [1]-[11] is the multicarrier modulation method in which a number of spectrally overlapping but coherently orthogonal modulated subcarriers are transmitted simultaneously. When compared with the single-carrier modulations using the same data rate, OFDM has been known to possess the prevailing features of high spectral efficiency and robustness against adverse channel effects including impulsive noise, intersymbol interference and multipath fading. Motivated by these prominent features, OFDM has been recently adopted as the modulation method in many broadband communication applications [12]-[14]. Most applications entail redundant block transmissions and enable efficient block processes to counteract the adverse channel effects, by inserting guard intervals with cyclic prefix (CP) [4]-[6] or zero padding (ZP) [7] between transmission blocks containing the useful data. Since the block processes can be practically implemented using the fast Fourier transform (FFT) algorithms [8], several applications have adopted a large number of multiplexed subcarriers (sometimes, hundreds) for embodying OFDM so that the above prevailing features are exploited to a large extent.

Although high spectral compactness can be achieved by OFDM with a large number of multiplexed subcarriers, pulse shaping is still of paramount importance to OFDM systems in that the subcarriers located near band edges are apt to interfere the adjacent channels when not properly shaped. Most of practical approaches use rectangular pulses [4]-[7] because such a pulse shape is very suitable for use in conjunction with redundant block transmissions and FFT processes. Unfortunately, the rectangularly pulsed OFDM has relatively

large power spectral sidelobes which fall off as  $f^{-2}$ , even with hundreds of subcarriers multiplexed. To minimize signal distortion over bandlimited channels and reduce power spillover into adjacent channels, the subcarriers at band edges are not modulated for most of applications [12]-[14], thus leaving the prominent OFDM feature of high spectral efficiency partially exploited. Although smoother pulses of finite duration [9]-[11] or infinite duration [1]-[3] have been suggested for OFDM, these different pulse shapes are not widely adopted in practice because implementation of FFT becomes either impossible or very complex (e.g., [3]) when the pulses other than the rectangular one are used.

Correlative coding is an efficient transmission technique exploited in the literature on bandlimited digital communications [15]-[17]. In methodology, correlative coding introduces memory or correlation to the transmitted data stream in time domain, in a way that the power spectrum of the transmitted bandlimited signal is shaped to exhibit gradual rolloff to band edges. This spectral property dramatically reduces the amount of excessive intersymbol interference at the receiver when the symbol timing is not perfectly synchronized. Operating on the data block in frequency domain, correlative coding has been recently applied in OFDM to suppress interchannel interference [18]-[19], reduce peak-to-average power ratio [20], and counteract channel effects [21]-[23]. Particularly, correlatively coded OFDM has been widely used to provide high degree of robustness against deep fades, and is much more popularly known as precoded OFDM in this context (see [21]-[22] and references therein). Despite these abundant applications, correlative coding is never used in OFDM for spectral shaping.

In the letter, correlative coding is adopted to shape the signal spectrum of the rectangularly pulsed OFDM signals with an attempt to achieve high spectral compactness. The proposed method is applicable to the rectangularly pulsed OFDM signals with or without zero padding or cyclic prefix. For convenience, the OFDM signals without guard intervals, with cyclic prefix and with zero padding are denoted by NG-OFDM, CP-OFDM and ZP-OFDM, respectively. The idea here is to introduce correlation to each data block before OFDM modulation via inverse FFT, in a way that the resultant power spectral sidelobes are made to decay very fast. To achieve fast decaying sidelobes, a class of correlative codes is proposed. It is analytically shown that the proposed  $L$ -th-order correlatively coded NG-OFDM and ZP-OFDM signals possess the prominent spectral property that the equivalent lowpass power spectral density (PSD) decays approximately with a rate  $f^{-2(L+1)}$  at spectral band edges, and thus exhibits very fast spectral rolloff at band edges even when  $L$  is a small positive integer. Particularly, much higher spectral compactness and

Manuscript received November 20, 2004; revised May 10, 2005 and July 23, 2005; accepted July 23, 2005. The associate editor coordinating the review of this paper and approving it for publication was A. Swami. This work was partially supported by the ROC National Science Council under Contracts 93-2213-E-008-014 and 94-2213-E-002-128.

C.-D. Chung is with the Graduate Institute of Communications Engineering and the Department of Electrical Engineering, National Taiwan University, Taipei, Taiwan 10617, Republic of China (email: cdchung@cc.ee.ntu.edu.tw).  
Digital Object Identifier 10.1109/TWC.2006.04794.

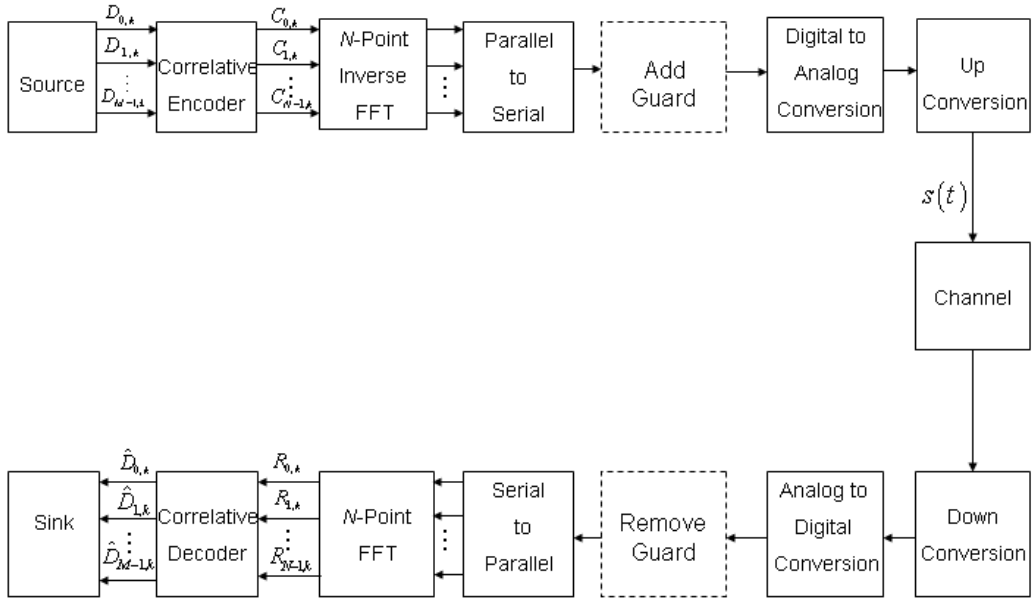


Fig. 1. System model.

efficiency than uncoded OFDM is numerically shown to be achieved by correlatively coded NG-OFDM, ZP-OFDM and CP-OFDM when a first-order or second-order correlative code is used.

## II. CORRELATIVELY CODED OFDM SIGNALS

Fig. 1 depicts the correlatively coded OFDM system. The memoryless OFDM source generates a block of  $M$  complex data symbols simultaneously and independently every  $T$  seconds, say  $\{D_{m,k}\}_{m=0}^{M-1}$  for the  $k$ -th signaling interval  $kT - T_g \leq t < kT + T_d$ , with  $T = T_d + T_g$ . Here,  $T_d$  and  $T_g$  represent the lengths of the time intervals for sending useful data symbols and for inserting cyclic prefix or padding zeros, respectively. All the data symbols  $D_{m,k}$ 's are assumed to be independent and identically distributed with zero mean and  $E\{|D_{m,k}|^2\} = 1$ . In the  $k$ -th signaling interval, the complex data symbol block  $\{D_{m,k}\}_{m=0}^{M-1}$  is first mapped into a block of  $N$  complex transmitted symbols  $\{C_{n,k}\}_{n=0}^{N-1}$  by the correlative encoding

$$C_{n,k} = \sum_{m=0}^{M-1} G_{n,m} D_{m,k} \quad n = 0, 1, \dots, N-1 \quad (1)$$

where  $G_{n,m}$ 's are complex encoder coefficients and  $N \geq M$  is assumed throughout. The encoder output symbols are then modulated in parallel with  $N$  subcarriers, equally spaced by  $\omega_d \triangleq 2\pi/T_d$ , and multiplexed to form the correlatively-coded OFDM signal as

$$s(t) = \rho \sum_k \operatorname{Re} \left\{ \sum_{n=0}^{N-1} C_{n,k} \cdot \exp\{j(\omega_0 + n\omega_d)(t - kT)\} \right\} p(t - kT) \quad (2)$$

where  $\rho$  is the signaling amplitude and  $\omega_0$  is the radian reference frequency with  $\omega_0 T \gg 1$ . The windowing function  $p(t)$  is a pulse defined on the time interval  $-T_g \leq t < T_d$ . If

$s(t)$  models the CP-OFDM signal,  $p(t)$  is a unit rectangular pulse over  $-T_g \leq t < T_d$ . If  $s(t)$  models the ZP-OFDM signal,  $p(t)$  is a unit rectangular pulse over  $0 \leq t < T_d$  and  $p(t) = 0$  over  $-T_g \leq t < 0$ . Note that the signal in the form of (2) can be realized by the  $N$ -point inverse FFT architecture as depicted in Fig. 1. By modeling so, the data symbol time  $T_s$  is related to the OFDM block length  $T$  by  $T_s = T/M$ .

Using (1),  $s(t)$  is rewritten as

$$s(t) = \rho \sum_{m=0}^{M-1} \sum_k \operatorname{Re} \{ D_{m,k} q_m(t - kT) \} \quad (3)$$

where  $q_m(t)$  is independent of data and defined by  $q_m(t) \triangleq \sum_{n=0}^{N-1} G_{n,m} \exp\{j(\omega_0 + n\omega_d)t\} p(t)$ . It is seen from (3) that  $s(t)$  is a multiplexing of  $M$  independent component signals which have zero mean. Moreover, each component signal carries a memoryless data stream and is orthogonal to its own  $lT$ -shifted version. It follows that the PSD of  $s(t)$  can be obtained from the multiplexing of  $M$  component signals bearing  $\{D_{m,k}\}_{m=0}^{M-1}$  for one specific  $k$ , say  $k = 0$ . Quoting [24, eq. 2.57], the PSD of  $s(t)$  is given by

$$S(f) = \frac{\rho^2}{4T} \sum_{m=0}^{M-1} \mathcal{E} \left\{ |D_{m,0} \mathcal{F}\{q_m(t)\} + D_{m,0}^* \mathcal{F}\{q_m^*(t)\}|^2 \right\} \quad (4)$$

where  $\mathcal{E}\{\cdot\}$  and  $\mathcal{F}\{\cdot\}$  represent expectation and Fourier transform, respectively. Since  $\omega_0 T \gg 1$ ,  $\mathcal{F}\{q_m(t)\}$  and  $\mathcal{F}\{q_m^*(t)\}$  contain virtually disjoint positive and negative spectral components, respectively. In the case, (4) simplifies to

$$S(f) = \frac{\rho^2}{4T} \sum_{m=0}^{M-1} \left\{ |\mathcal{F}\{q_m(t)\}|^2 + |\mathcal{F}\{q_m^*(t)\}|^2 \right\}. \quad (5)$$

It follows that the equivalent lowpass PSD's for CP-OFDM

and ZP-OFDM are obtained as

$$S_{LP}^{CP}(f) = \frac{\rho^2 T}{2} \sum_{m=0}^{M-1} \left| \sum_{n=0}^{N-1} g_{n,m} \cdot \text{sinc}\left(\left(n - \frac{N-1}{2}\right) \frac{T}{T_d} - fT\right) \right|^2 \quad (6)$$

$$S_{LP}^{ZP}(f) = \frac{\rho^2 T_d^2}{2T} \sum_{m=0}^{M-1} \left| \sum_{n=0}^{N-1} g_{n,m} \cdot \text{sinc}\left(n - \frac{N-1}{2} - fT_d\right) \right|^2 \quad (7)$$

where  $\text{sinc}(x) \triangleq \sin(\pi x)/(\pi x)$  is the sampling function, and  $g_{n,m}$ 's are related to  $G_{n,m}$ 's by  $g_{n,m} \triangleq \zeta_n G_{n,m}$  with  $\zeta_n = \exp\{j\frac{n}{2}\omega_d(T_d - T_g)\}$  for CP-OFDM and  $\zeta_n = (-1)^n$  for ZP-OFDM. Further, the transmission signal power  $P$  is given by  $P = \frac{\rho^2}{2} \sum_{m=0}^{M-1} \sum_{n=0}^{N-1} \sum_{l=0}^{N-1} g_{n,m} g_{l,m}^* \text{sinc}\left(\left(n-l\right) \frac{T}{T_d}\right)$  for CP-OFDM and  $P = \frac{\rho^2 T_d}{2T} \sum_{m=0}^{M-1} \sum_{n=0}^{N-1} |g_{n,m}|^2$  for ZP-OFDM.

When  $T_g = 0$ , both CP-OFDM and ZP-OFDM signals reduce to the same NG-OFDM signal, which has the equivalent lowpass PSD

$$S_{LP}^{NG}(f) = \frac{PT}{\sum_{m=0}^{M-1} \sum_{n=0}^{N-1} |g_{n,m}|^2} \cdot \sum_{m=0}^{M-1} \left| \sum_{n=0}^{N-1} g_{n,m} U\left(\frac{N-1}{2} + fT; 0, n\right) \right|^2 \quad (8)$$

where we set  $g_{n,m} = \zeta_n G_{n,m}$  with  $\zeta_n = (-1)^n$ . Note that the convenient notation  $U(x; 0, n)$  is adopted to represent the sampling function as  $U(x; 0, n) \triangleq \text{sinc}(n - x)$ ,  $n = 0, 1, \dots$

In the letter, we consider a special family of correlative codes which are characterized by  $G_{n,m} = 0$  for  $n \notin \{m, m+1, \dots, m+L\}$ , where we set  $L = N - M$ . From (1), such correlative encoders produce the transmitted symbol block  $\{C_{n,k}\}_{n=0}^{N-1}$  by convolving the data symbol block  $\{D_{m,k}\}_{m=0}^{M-1}$  with the finite-length complex response  $\{G_{m+l,m}; l = 0, 1, \dots, L\}_{m=0}^{M-1}$  and can be regarded as a complex filter in frequency domain. This type of correlative encoders generally increases the complexity of the baseband OFDM transmitter with an order linearly proportional to  $M(L+1)$ . Clearly, there are various choices of the filter and one may choose the complex response optimally so as to meet certain criterion on the signal spectrum. The optimal design of the filter is, however, beyond the scope of the letter and left as an open issue. Instead, a particular class of correlative codes is proposed as follows.

Specifically, the proposed correlative codes are characterized by  $g_{n,m} = \tilde{g}_{n-m}$  for all  $n$  and  $m$  with  $\tilde{g}_l$  defined by  $\tilde{g}_l = \left(\frac{L}{l}\right)$ ,  $l = 0, 1, \dots, L$ , and  $\tilde{g}_l = 0$  otherwise. When  $L = 0$ , the signal (2) simplifies to the uncoded rectangularly pulsed OFDM signal whose power spectral sidelobes fall off as  $f^{-2}$ , as clearly indicated by (6), (7) and (8). When  $L$  is a positive integer, we conveniently denote  $\mathcal{G}_L$  as the  $L$ -th order correlative code characterized by  $\{\tilde{g}_l\}_{l=0}^L$ . To demonstrate the spectral advantage achieved by  $\mathcal{G}_L$ , a new function set containing  $U(x; 0, n)$ 's is introduced below.

A) A New Function Set  $\{U(x; m, n); m, n=0, 1, \dots\}$ : Define the real-valued function  $U(x; m, n)$  for any real  $x$  and nonnegative integers  $m$  and  $n$  as

$$U(x; m, n) \triangleq \pi^{-1} m! \sin(\pi(n-x)) \prod_{k=0}^m (n+k-x)^{-1}. \quad (9)$$

The function set  $\{U(x; m, n); m, n = 0, 1, \dots\}$  satisfies the following properties.

*Property 1:* When  $x$  and  $n$  are given,  $U(x; m, n)$ 's satisfy the recursion  $U(x; m, n) = U(x; m-1, n) + U(x; m-1, n+1)$ ,  $m = 1, 2, \dots$

*Property 2:* When  $x$  and  $n$  are given,  $U(x; m, n)$  is a linear combination of  $U(x; 0, n+l)$  for  $l = 0, 1, \dots, m$  as  $U(x; m, n) = \sum_{l=0}^m \binom{m}{l} U(x; 0, n+l)$ ,  $m = 1, 2, \dots$

*Property 3:* When  $m$  and  $n$  take finite values,  $U^2(x; m, n)$  varies proportionally with  $x^{-2(m+1)}$  as  $|x|$  approaches to infinity.

Based on (9), *Property 1* can be readily proven by induction and used in turn to induce *Property 2*. *Property 3* follows directly from the definition (9).

B) Spectral Property and Performance of  $\mathcal{G}_L$ -Coded OFDM Signals: Using  $\mathcal{G}_L$ , (8) becomes

$$S_{LP}^{NG}(f) = \frac{PT}{M \sum_{l=0}^L \binom{L}{l}^2} \cdot \sum_{m=0}^{M-1} \left| \sum_{l=0}^L \binom{L}{l} U\left(\frac{N-1}{2} + fT; 0, m+l\right) \right|^2 = \frac{PT}{M \binom{2L}{L}} \sum_{m=0}^{M-1} U^2\left(\frac{N-1}{2} + fT; L, m\right) \quad (10)$$

where the second equality is obtained by quoting *Property 2* and the identity  $\sum_{l=0}^L \binom{L}{l}^2 = \binom{2L}{L}$ . When  $M, N$  and  $L$  take finite values, it is seen from *Property 3* that  $S_{LP}^{NG}(f)$  varies proportionally with  $|fT|^{-2(L+1)}$  as  $|fT|$  approaches to infinity. This implies that the signal spectrum for the  $\mathcal{G}_L$ -coded NG-OFDM signal exhibits faster rolloff at spectral sidelobes when  $L$  is increased. Therefore, the  $\mathcal{G}_L$ -coded NG-OFDM signal is expected to yield higher spectral compactness and efficiency than the conventional uncoded NG-OFDM signal, especially when  $L$  is large. The same comment also applies to the  $\mathcal{G}_L$ -coded ZP-OFDM signal because  $S_{LP}^{ZP}(f)$  has the exact form of (10) with  $T$  replaced by  $T_d$ .

In what follows, the spectral compactness is characterized by the fractional out-of-band power

$$\eta = 10 \log_{10} \left( 1 - \frac{1}{P} \int_{-B/2}^{B/2} S_{LP}(f) df \right) \quad (11)$$

which denotes the fraction of total power that is not captured within the frequency band  $[-B/2, B/2]$ . In particular, the spectral trends on  $\eta$  for various signals are studied with respect to the normalized bandwidth  $BT_s$  so that the spectral efficiency can be compared among different signals with the same data symbol rate. Here, the spectral efficiency is referred

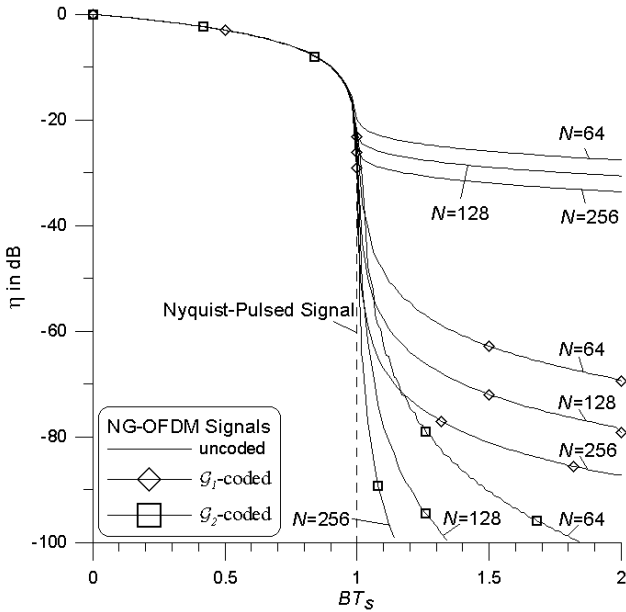


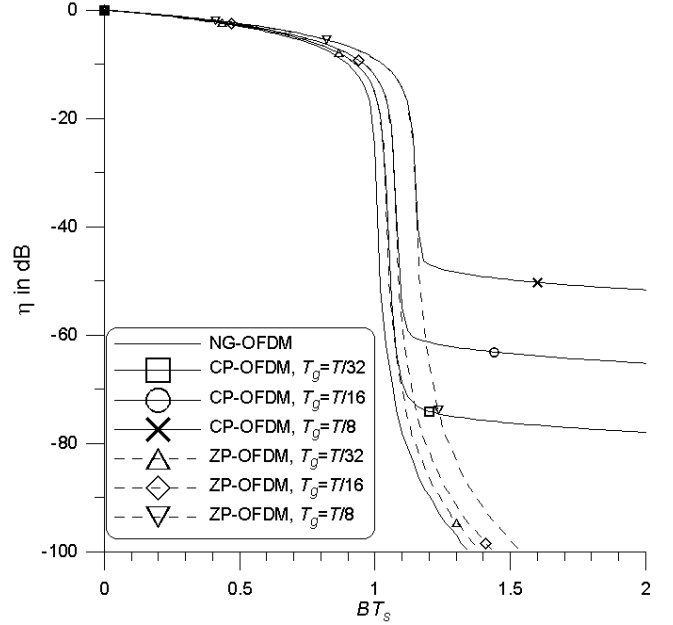
Fig. 2. Fractional out-of-band power characteristics of NG-OFDM signals.

to as the inverse of  $BT_s$  that is required to achieve a given  $\eta$ . Therefore, to achieve a fixed  $\eta$ , the signal requiring a smaller  $BT_s$  can exhibit higher spectral efficiency.

Fig. 2 compares the spectral efficiencies of various  $\mathcal{G}_L$ -coded and uncoded NG-OFDM signals with  $N$  and  $L$  varied. As a benchmark, the ideal performance of the single-carrier Nyquist-pulsed signal with  $\mathcal{S}_{LP}(f) = T_s$  if  $|f| < 1/(2T_s)$  and  $\mathcal{S}_{LP}(f) = 0$  otherwise is also plotted for comparison. Several trends can be observed on the achievable spectral efficiency when the required  $\eta$  is small (say, less than  $-20$  dB). First, the spectral efficiencies of uncoded and coded NG-OFDM are shown to improve as  $N$  is increased. The improvement is, however, only moderate for uncoded NG-OFDM, but rather significant for  $\mathcal{G}_L$ -coded NG-OFDM. Second, when  $N$  is fixed,  $\mathcal{G}_L$ -coded NG-OFDM improves significantly over uncoded NG-OFDM in spectral efficiency. The improvement is large when  $\mathcal{G}_1$  is used and increases as a higher coding order is adopted. Third,  $\mathcal{G}_L$ -coded NG-OFDM can provide very high spectral efficiency even when the required  $\eta$  is extremely small. For example, the normalized bandwidth  $BT_s$  required to achieve  $\eta = -80$  dB is given by around 1.44, and 1.05 for  $\mathcal{G}_1$ -coded and  $\mathcal{G}_2$ -coded NG-OFDM with  $N = 256$ , respectively, but is enormously large for uncoded NG-OFDM. Last, the ideal Nyquist performance is closely approached by the  $\mathcal{G}_2$ -coded NG-OFDM signal with  $N = 256$ , even when the required  $\eta$  is extremely small.

Observe (7) for ZP-OFDM. When the same  $\mathcal{G}_L$ ,  $M$ ,  $N$  and  $T$  are used, the  $\mathcal{S}_{LP,1}^{ZP}(f)$  of ZP-OFDM using  $T_{d,1}$  is related to the  $\mathcal{S}_{LP,2}^{ZP}(f)$  of ZP-OFDM using  $T_{d,2}$  by  $\mathcal{S}_{LP,1}^{ZP}(f/T_{d,1})/T_{d,1} = \mathcal{S}_{LP,2}^{ZP}(f/T_{d,2})/T_{d,2}$ . Using this in (11) reveals that the ZP-OFDM signal using  $T_d$  exhibits  $(T_d/T)$ -fold the spectral efficiency of the NG-OFDM signal, provided that both signals are based on the same  $\mathcal{G}_L$ ,  $M$ ,  $N$  and  $T$ . Thus, the results in Fig. 2 also apply to ZP-OFDM with the spectral efficiencies rescaled by a factor  $T_d/T$ .

Due to the use of guard intervals, both ZP-OFDM and CP-


 Fig. 3. Fractional out-of-band power characteristics of  $\mathcal{G}_2$ -coded CP-OFDM and ZP-OFDM signals with  $N = 128$ .

OFDM degrade from NG-OFDM in spectral efficiency. The longer the guard interval, the more severe the degradation. This performance trend is clearly illustrated in Fig. 3, where the  $\mathcal{G}_2$ -coded ZP-OFDM and CP-OFDM signals with various  $T_g/T$  ratios is compared with the corresponding NG-OFDM. It is also shown that ZP-OFDM outperforms CP-OFDM for the same  $T_g/T$  ratio when the required  $\eta$  is extremely small (say,  $-80$  dB). Despite of the degradation from NG-OFDM, very high spectral efficiency relative to a small required  $\eta$  (say,  $-40$  dB) can still be achieved by  $\mathcal{G}_2$ -coded CP-OFDM and ZP-OFDM, even though  $T_g/T$  is as high as up to  $1/8$ .

Because  $M$  data symbols are transmitted on  $N$  subcarriers every  $T$  seconds, the data rate provided by  $\mathcal{G}_L$ -coded OFDM is  $M/N$ -fold the rate provided by uncoded OFDM. The loss is, however, negligible when  $N \gg L$ .<sup>1</sup> Even with this loss in data rate,  $\mathcal{G}_L$ -coded OFDM can provide much higher spectral efficiency than uncoded OFDM when a very small out-of-band power is required.

The in-band spectrum flatness is also of practical interest in the design of passband filtering. Table I illustrates the in-band flatness characteristics of uncoded and correlatively coded NG-OFDM and CP-OFDM, in which the flatness measure  $\lambda_X$  is defined by the maximum-to-minimum PSD ratio within the normalized bandwidth  $X$ , i.e.,  $\lambda_X \triangleq \max_{|f| \leq X/(2T_s)} \mathcal{S}_{LP}(f) / \min_{|f| \leq X/(2T_s)} \mathcal{S}_{LP}(f)$ . When  $N$  is large enough,  $\mathcal{G}_L$ -coded signals are shown to provide relatively flat in-band spectrum in comparison with uncoded signals.

### III. MAXIMUM-LIKELIHOOD BLOCK DECODING

Assuming that the receiver is perfectly synchronized in amplitude, frequency, phase and timing to the received signal,

<sup>1</sup>Dictated by the operating channel characteristics and the affordable transceiver complexity, large FFT sizes with  $N \geq 64$  have been chosen in most contemporary applications [12]-[14]. In the case, the constraint  $N \gg L$  is satisfied for a small coding order  $L$ .

TABLE I  
IN-BAND FLATNESS CHARACTERISTICS OF (A) NG-OFDM AND (B)  
CP-OFDM WITH  $T_g = T/8$

NG-OFDM Scheme	$\lambda_{0.99}$ (in dB)		
	$N = 64$	$N = 128$	$N = 256$
uncoded	0.449	0.43	0.213
$\mathcal{G}_1$ -coded	1.029	0.1866	0.01896
$\mathcal{G}_2$ -coded	1.405	0.5013	0.00946

(a)

CP-OFDM Scheme	$\lambda_{1.132}$ (in dB)		
	$N = 64$	$N = 128$	$N = 256$
uncoded	2.451	2.441	2.298
$\mathcal{G}_1$ -coded	1.297	0.3558	0.1245
$\mathcal{G}_2$ -coded	1.446	0.5531	0.02326

(b)

the  $\mathcal{G}_L$ -coded OFDM signals can be coherently decoded, by applying the maximum-likelihood (ML) method on each received useful signal block. To exemplify the approach, we consider here the  $\mathcal{G}_L$ -coded OFDM signal with  $J^2$ -ary quadrature amplitude modulation (QAM) component modulations and present the coherent ML decoding approach operating separately in inphase ( $I$ ) and quadrature-phase ( $Q$ ) channels.

Denote  $\{R_{n,k}^{(x)}\}_{n=0}^{N-1}$  as the  $x$ -channel FFT output block at the receiver for the  $k$ -th signaling interval, with  $x = I$  and  $Q$ , where  $R_{n,k}^{(x)}$  is the received real-valued symbol on the  $n$ -th subcarrier, defined by  $R_{n,k}^{(x)} = \alpha_n C_{n,k}^{(x)} + W_{n,k}^{(x)}$ . Here,  $\{C_{n,k}^{(x)}\}_{n=0}^{N-1}$  is the  $\mathcal{G}_L$ -coded symbol block composed by correlatively encoding the  $x$ -channel block of pulse amplitude modulated data symbols  $\{D_{m,k}^{(x)}\}_{m=0}^{M-1}$ , with  $D_{m,k}^{(x)} \in \{\pm\beta, \pm 3\beta, \dots, \pm(J-1)\beta\}$  and  $\beta = (3/(2J^2 - 2))^{1/2}$ , as  $C_{n,k}^{(x)} = \sum_{m=\max\{0, n-L\}}^{\min\{M-1, n\}} \binom{L}{n-m} D_{m,k}^{(x)}$ .  $\alpha_n$  is the channel

amplitude on the  $n$ -th subcarrier.  $\{W_{n,k}^{(x)}\}_{n=0}^{N-1}$  are the additive white Gaussian noise (AWGN) samples which are independent and identically distributed over different channels and subcarriers with zero mean. Based on  $\{R_{n,k}^{(x)}\}_{n=0}^{N-1}$ , the ML block decoding rule is to find  $\{\hat{D}_{m,k}^{(x)}\}_{m=0}^{M-1}$  which yields the minimum squared Euclidean distance,

$$\{\hat{D}_{m,k}^{(x)}\}_{m=0}^{M-1} = \min_{\{D_{m,k}^{(x)}\}_{m=0}^{M-1}} \sum_{n=0}^{N-1} |R_{n,k}^{(x)} - \alpha_n \sum_{m=\max\{0, n-L\}}^{\min\{M-1, n\}} \binom{L}{n-m} D_{m,k}^{(x)}|^2. \quad (12)$$

This rule is optimum in the sense that the probability of error in coherently decoding each data block is minimized. Since the squared distance metric is additive over the index  $n$ , the decoding rule can be efficiently realized by the Viterbi algorithm [24] which computes the partial squared distance sums progressively over  $n$ . Such realization increases the complexity of the baseband OFDM receiver with an order linearly proportional to  $J^L N$ .

Fig. 4 gives the simulated bit error rate (BER) results of the coherent ML block decoding of Gray-labeled  $\mathcal{G}_L$ -coded

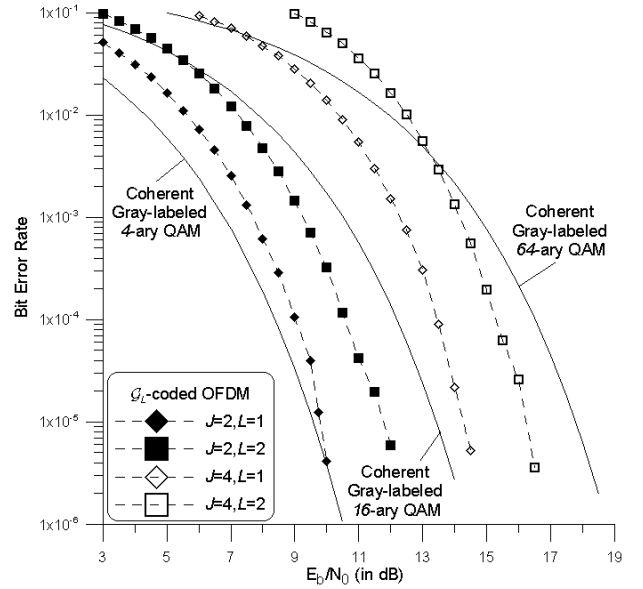


Fig. 4. Bit error rate characteristics of Gray-labeled  $\mathcal{G}_L$ -coded NG-OFDM with  $N = 64$ ,  $J^2$ -ary QAM component modulation and coherent ML block decoding on the AWGN channel.

NG-OFDM with  $J^2$ -ary QAM component modulations on the AWGN channel with flat channel gains (i.e.,  $\alpha_n = \alpha$  for all subcarriers). The analytical results of the coherent uncoded Gray-labeled  $J^2$ -ary QAM schemes [24] are also plotted for comparison. As indicated,  $\mathcal{G}_L$ -coded NG-OFDM degrades by a few decibels from the corresponding  $J^2$ -ary QAM. The larger the coding order, the worse the degradation in error performance. This degradation results from the signaling characteristic that more signaling levels are transmitted by  $\mathcal{G}_L$ -coded OFDM versus uncoded OFDM. Furthermore, when  $L$  is increased, there is a concomitant increase in BER degradation and in system complexity. Both BER degradation and complexity increase turn out to be major tradeoffs to the prominent spectral property achieved by correlatively coded OFDM.

As indicated by (12), the ML block decoding can equalize the effects of delay-spread fading (i.e.,  $\alpha_n$ 's may be different) and correlative encoding simultaneously.<sup>2</sup> Fig. 5 illustrates the simulated BER results of Gray-labeled  $\mathcal{G}_L$ -coded CP-OFDM with 4-ary QAM component modulations on two typical delay-spread channels defined in [21]. The CP length is assumed to be long enough so as to reject the intersymbol interference. The channel amplitudes are given by  $\alpha_n = |H(z)|_{z=\exp\{j2n\pi/N\}}$  where the channel transfer function  $H(z)$  is defined by  $H(z) = 0.407 + 0.815z^{-1} + 0.407z^{-2}$  for Channel A and  $H(z) = 0.8 + 0.6z^{-1}$  for Channel B. Note in [21] that Channel A is a three-tap spectral-null channel while Channel B is a two-tap channel which has no spectral null but small channel amplitudes at some subcarriers. Due to correlative coding,  $\mathcal{G}_L$ -coded CP-OFDM suffers performance loss from uncoded CP-OFDM in Channel B and the loss increases as the coding order increases. In Channel A, performance loss due to correlative coding is not

<sup>2</sup>Although the delay-spread channel effect is equalized, ML block decoding increases the system complexity and, particularly, loses the simplicity of one-tape zero-forcing equalization which is widely used in uncoded OFDM systems.

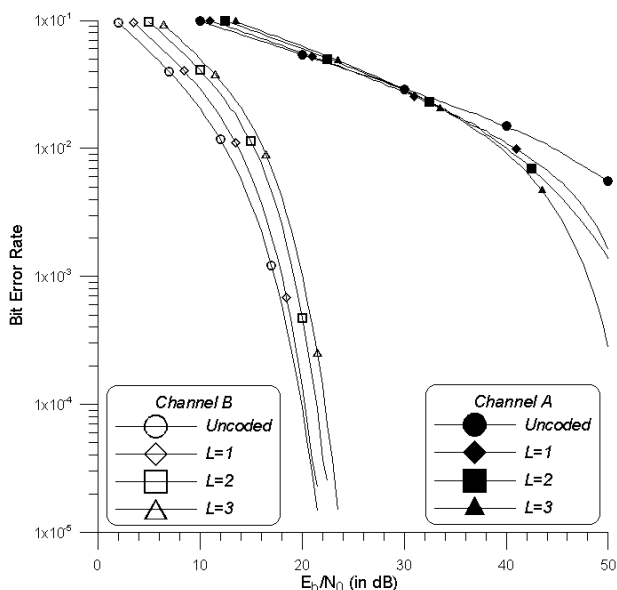


Fig. 5. Bit error rate characteristics of Gray-labeled  $\mathcal{G}_L$ -coded CP-OFDM with  $N = 64$ , 4-ary QAM component modulation and coherent ML block decoding on delay spread channels.

significant and, contrarily,  $\mathcal{G}_L$ -coded CP-OFDM noticeably outperforms uncoded CP-OFDM in the low BER regions. This primarily results from the signaling characteristic that correlative coding over  $L + 1$  consecutive subcarriers permits the ML block decoding and, thereby, guarantees additional robustness against the three-tap spectral-null channel where at worst two sub-carriers coincide with channel nulls. Therefore, when used to combat the  $(I + 1)$ -tap spectral-null channels, the coding order  $L$  can be chosen not smaller than  $I$  so as to guarantee high spectral compactness and robustness against channel nulls simultaneously.

Although error performance is traded off due to correlative coding for some channels, such performance loss can be, however, easily compensated for by applying appropriate transmission methods. For example, one can apply error-correcting codes temporally (perhaps, in conjunction with interleaving on frequency domain) over different OFDM blocks or diversity combining spatially over multiple antennas to correlative coded OFDM, so that the overall system error performance is satisfactory while very fast decaying spectral rolloff at band edges is simultaneously retained.<sup>3</sup>

#### IV. CONCLUSION

In the letter, the correlative coded OFDM format is proposed to significantly improve the spectral efficiency of the rectangularly pulsed OFDM signal with or without cyclic prefix or zero padding, in a way that the required fractional out-of-band power can be made extremely small. Although

<sup>3</sup>As pointed out by an anonymous reviewer, there are  $L + 1$  data symbols embedded in each subcarrier on frequency  $\omega_0 + n\omega_d$  for  $n \in \{L, L + 1, \dots, N - L - 1\}$ , but less data symbols embedded in each subcarrier on frequency  $\omega_0 + n\omega_d$  for  $n \in \{0, 1, \dots, L - 1\}$  and  $n \in \{N - L, N - L + 1, \dots, N - 1\}$ . This indicates unequal information protection among data symbols. This unequal information protection may impact the overall system error performance and, thus, different care may have to be taken of among data symbols located on different frequency positions when error-correcting codes are temporally applied.

the error performance is traded off for some channels due to correlative coding, the proposed signaling format is promising for use in bandlimited applications, where powerful coding or diversity schemes in temporal or spatial domains are used in conjunction with rectangularly pulsed OFDM to provide high spectral and power efficiencies simultaneously.

#### REFERENCES

- [1] R. W. Chang, "Synthesis of band-limited orthogonal signals for multi-channel data transmission," *Bell Syst. Tech. J.*, vol. 45, pp. 1775-1796, Dec. 1966.
- [2] B. R. Saltzberg, "Performance of an efficient parallel data transmission system," *IEEE Trans. Commun. Technol.*, vol. 15, pp. 805-811, Dec. 1967.
- [3] B. Hirosaki, "An orthogonally multiplexed QAM system using the discrete Fourier transform," *IEEE Trans. Commun.*, vol. 29, pp. 982-989, July 1981.
- [4] J. A. C. Bingham, "Multicarrier modulation for data transmission: An idea whose time has come," *IEEE Commun. Mag.*, vol. 28, no. 5, pp. 5-14, May 1990.
- [5] S. H. Müller-Weinfurtner, "Optimum Nyquist windowing in OFDM receivers," *IEEE Trans. Commun.*, vol. 49, pp. 417-420, Mar. 2001.
- [6] K. Zhong, T. Tjhung, and F. Adachi, "A general SER formula for an OFDM system with MDPSK in frequency domain over Rayleigh fading channels," *IEEE Trans. Commun.*, vol. 52, pp. 584-594, Apr. 2004.
- [7] B. Muquet, Z. Wang, G. B. Giannakis, M. de Courville, and P. Duhamel, "Cyclic prefixing or zero padding for wireless multicarrier transmissions?" *IEEE Trans. Commun.*, vol. 50, pp. 2136-2148, Dec. 2002.
- [8] C. D. Murphy, "Low-complexity FFT structures for OFDM transceivers" *IEEE Trans. Commun.*, vol. 50, pp. 1878-1881, Dec. 2002.
- [9] R. Li and G. Stette, "Time-limited orthogonal multicarrier modulation schemes," *IEEE Trans. Commun.*, vol. 43, pp. 1269-1272, Feb./Mar./Apr. 1995.
- [10] L. Wei and C. Schlegel, "Synchronization requirements for multi-user OFDM on satellite mobile and two-path Rayleigh fading channels," *IEEE Trans. Commun.*, vol. 43, pp. 887-895, Feb./Mar./Apr. 1995.
- [11] A. Vahlin and N. Holte, "Optimal finite duration pulses for OFDM," *IEEE Trans. Commun.*, vol. 44, pp. 10-14, Jan. 1996.
- [12] ANSI, "Network and consumer installation interfaces-Asymmetric digital subscriber line (ADSL) metallic interface," 1995.
- [13] ETSI, "Digital video broadcasting (DVB-T): framing structure, channel coding and modulation for digital terrestrial television," ETS 300 744, Dec. 2001.
- [14] IEEE, "Wireless LAN medium access control (MAC) and physical layer (PHY) specifications: higher speed physical layer (PHY) extension in the 5GHz band," IEEE Std. 802.11a/D5.0, Apr. 1999.
- [15] A. Lender, "The duobinary technique for high speed data transmission," *IEEE Trans. Commun. Electron.*, vol. 82, pp. 213-218, May 1963.
- [16] H. Kobayashi, "Correlative level coding and maximum-likelihood decoding," *IEEE Trans. Inf. Theory*, vol. 17, pp. 586-594, Sep. 1971.
- [17] P. Galiko and S. Pasupathy, "Linear receivers for correlative coded MSK," *IEEE Trans. Commun.*, vol. 33, pp. 338-347, Apr. 1985.
- [18] Y. Zhao, J. D. Leclercq, and S. G. Häggman, "Intercarrier interference compression in OFDM communication systems by using correlative coding," *IEEE Commun. Lett.*, vol. 2, no. 8, pp. 214-216, Aug. 1998.
- [19] A. N. Husna, S. Y. S. Kamilah, B. Ameruddin, and E. Mazlina, "Intercarrier interference (ICI) analysis using correlative coding OFDM system," in *Proc. 2004 RF and Microwave Conf.*, pp. 235-237.
- [20] S. K. Yusof and N. Faisal, "Correlative coding with clipping and filtering technique in OFDM systems," in *Proc. ICICS-PCM Conf. 2003*, pp. 1456-1459.
- [21] X. G. Xia, "Precoded and vector OFDM robust to channel spectral nulls and with reduced cyclic prefix length in single transmit antenna systems," *IEEE Trans. Commun.*, vol. 49, pp. 1363-1374, Aug. 2001.
- [22] Z. Wang, S. Zhou, and G. B. Giannakis, "Joint coding-precoding with low-complexity turbo-decoding," *IEEE Trans. Wireless Commun.*, vol. 3, pp. 832-842, May 2004.
- [23] M. Debbah, P. Loubaton, and M. de Courville, "Asymptotic performance of successive interference cancellation in the context of linear precoded OFDM systems," *IEEE Trans. Commun.*, vol. 52, pp. 1444-1448, Sept. 2004.
- [24] M. K. Simon, S. M. Hinedi, and W. C. Lindsey, *Digital Communication Techniques*. Englewood Cliffs, NJ: Prentice Hall, 1994.